**TREE-RING RESEARCH,** *Vol. 78(2), 2022, pp. 113–128*
DOI: https://doi.org/10.3959/2021-20

# DENDROCLIMATOLOGY OF YELLOW-CEDAR (*CALLITROPSIS NOOTKATENSIS*) AND TEMPERATURE VARIABILITY ON THE WESTERN SLOPES OF THE NORTH CASCADES IN WASHINGTON STATE, USA, FROM 1333 TO 2015 CE

**CHRISTOPHER A. TRINIES[1], ANDREW G. BUNN[1*], CHRISTOPHER S. ROBERTSON[1],** and **KEVIN J. ANCHUKAITIS[2]**

[1]Department of Environmental Sciences, Western Washington University, Bellingham, WA, USA

[2]Laboratory of Tree-Ring Research, and School of Geography, Development, and Environment, University of Arizona, Tucson, AZ, USA

## ABSTRACT

Long-term paleoclimate reconstructions of temperature provide context for the magnitude of recent anthropogenic warming, help quantify the climate response to radiative forcing, and better characterize the range of natural variability. In North America, temperature-sensitive tree-ring proxy data remain sparse, which limits the spatial and temporal extent of these reconstructions. Here we present an analysis of yellow-cedar (*Callitropsis nootkatensis*) growth in Washington State (USA) and its relationship to climate. Combining empirical statistical analysis with a process model of xylogenesis, we show that tree-ring chronologies from three high-elevation sites in the North Cascades are primarily controlled by temperature. We then use these chronologies to reconstruct summer temperatures over the period 1333 to 2015 CE, adding a new proxy to the North American network of temperature-sensitive trees. Comparison with an existing large-scale spatial gridded reconstruction suggests this species offers important local and regional information on past temperatures.

*Keywords:* tree rings, temperature network, temperature reconstruction, forward modeling, climate change.

## INTRODUCTION

Paleoclimate proxy data provide essential information for better understanding the dynamics and range of climate variability so that societies can plan for, adapt to, and mitigate against anthropogenic global warming and its consequences (Anchukaitis 2017). Proxy data from tree rings that span the late Holocene provide evidence for and advanced understanding of how the climate has evolved over the Common Era, including at hemispheric and even global scales. Reconstruction of past climates have provided valuable insights into the relative importance of natural and anthropogenic climate forcings and help evaluate the models used for projections of future climate (Hegerl *et al*. 2006; Schurer *et al.* 2014). Paleoclimate data can also be used to infer past atmospheric and ocean circulation on timescales from decades to centuries and how these may contribute to spatiotemporal patterns of climate variability (*e.g.* Ault *et al.* 2013; Cobb *et al.* 2013; Emile-Geay *et al.* 2013; Coats *et al.* 2016; Hernández *et al.* 2020; Power *et al.* 2021).

The majority of tree-ring chronologies are moisture-sensitive, however (St. George 2014; Consortium 2017), and the network of sites useful for temperature reconstruction are still quite limited, particularly in North America (Trouet *et al.* 2013; Esper *et al.* 2016; Wilson *et al.* 2016; Anchukaitis *et al.* 2017; Guillet *et al.* 2017; Esper *et al.* 2018; Martin *et al.* 2020). When local proxies are not available, reconstructions may be based on data from distal proxy sites. Although temperature anomalies can be autocorrelated over hundreds of kilometers and therefore conserved over large areas (Jones and Briffa 1992; Briffa and Jones 1993; Wettstein *et al.* 2011), areas of mountainous ter-

*Corresponding author: bunna@wwu.edu

rain can also exhibit complex and differing climate expression at local scales (Bunn *et al.* 2018). This can then result in an estimate of local or regional climate that might or might not reflect the true range of variation in climate over time and a reconstruction that might remain skillful at hemispheric scales but not capture important features at finer scales.

For example, recent tree-ring based reconstruction of Northern Hemisphere summer temperatures (Schneider *et al.* 2015; Stoffel *et al.* 2015; Wilson *et al.* 2016; Anchukaitis *et al.* 2017; Guillet *et al.* 2017; King *et al.* 2021) use relatively small but highly temperature-sensitive networks of tree-ring width, latewood density, and blue intensity. However, the number of North American sites is small and large portions of North America are represented by only one or two proxy chronologies, particularly prior to 1200 CE. There are therefore large spatial gaps between tree-ring proxy sites, which limits finer-scale understanding of regional climate variability and will negatively impact the skill of spatial reconstructions as a whole despite the tendency for temperature anomalies to be spatially autocorrelated.

The Pacific Northwest (PNW) of the conterminous United States is one such area where we know comparatively little about the local temperature variability over the last millennium, particularly west of the Cascade Mountains. The lack of long temperature proxies in the region stems in part from the climate diversity within a small spatial extent. Proximity to the Pacific Ocean acts to buffer temperatures west of the Cascades, leading to a smaller diurnal and seasonal temperature variations than those experienced on the eastern slopes or other areas influenced by a continental climate regime (Franklin and Dyrness 1973). The Cascades also provide a topographic break between the mesic coast and dry eastern interior. Lowland precipitation on the western side of the Cascade divide is itself often moderated by the rainshadow cast by the coastal Olympic Mountains. As a result of these climate and ecological conditions, there are many excellent moisture-sensitive tree-ring proxy records in the water-limited eastern part of the region (*e.g.* Brubaker 1980; Graumlich 1987; Littell *et al.* 2016; Dannenberg and Wise 2016). At high elevations in the Cascades, where temperature-limited growing conditions might be expected (Fritts 1966; Körner 2012), winter snowpack is often at least as strong of a factor in limiting growth as summer temperatures (Peterson and Peterson 2001; Harley *et al.* 2020; Coulthard *et al.* 2021). The result is that large scale temperature reconstructions in the Pacific Northwest are thus far represented by proxies from either higher latitudes or further to the east toward the continental interior, where temperatures more reliably limit summer growth.

It is therefore a considerable but important challenge to find additional suitable proxy data for temperature variations in the region, and prior research here has not been able to consistently separate the influence of winter snowpack from summer temperatures on annual tree growth. Most of the high-elevation species that have been studied, including mountain hemlock (*Tsuga mertensiana* (Bong.) Carrière), Pacific silver fir (*Abies amabilis* Douglas ex Loudon), subalpine fir (*Abies lasiocarpa* (Hook.) Nutt.), lodgepole pine (*Pinus contorta* Douglas ex Loudon), and subalpine larch (*Larix lyallii* Parl.) show a temperature sensitivity in ring width that is heavily moderated by either winter snowpack or growing-season moisture availability (Graumlich and Brubaker 1986; Peterson and Peterson 2001; Peterson *et al.* 2002; Case and Peterson 2007; Coulthard *et al.* 2021; Kemp-Jennings *et al.* 2021). Douglas-fir (*Pseudotsuga menziesii* (Mirib.) Franco.) and ponderosa pine (*Pinus ponderosa* P. Lawson & C. Lawson), two other common species in the region, tend to exhibit a sensitivity to water availability without the temperature relationship, or with a negative relationship to summer temperatures that is more indicative of water stress (Littell *et al.* 2008; Kusnierczyk and Ettl 2002). Where a temperature reconstruction has been attempted, it has necessarily involved a relatively complicated process using multiple species to separate out the temperature signal from the others (*e.g.* Graumlich and Brubaker 1986), which potentially compounds uncertainties.

One species that has shown sensitivity to summer temperatures without the winter precipitation limitation is yellow-cedar (*Callitropsis nootkatensis* (D. Don) D. P. Little), but that species has not been intensively used for climate reconstructions in the southern part of its range (Laroque and Smith 1999; Wiles *et al.* 2019), in part because of complex climate/growth relationships. For in-

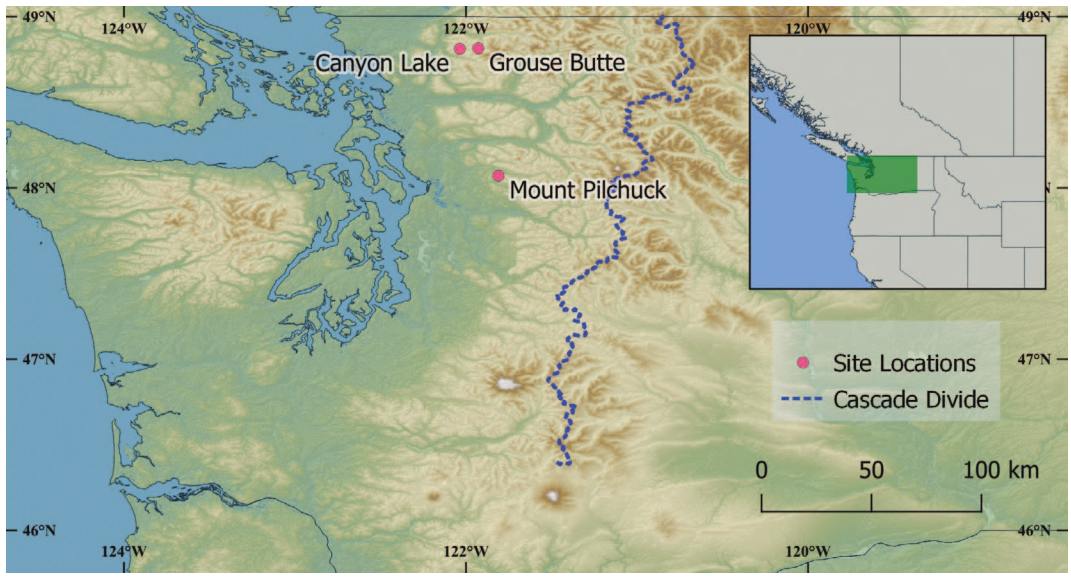


**Figure 1.** Site locations within the Washington Cascades. Yellow-cedar chronologies were built at each of the three sites: Canyon Lake (UCL), Grouse Butte (GRO) and Mount Pilchuck (PIL).

stance, Wiles *et al.* (2012) identified non-stationary climate/growth relationships in healthy yellow-cedar stands at low-elevation sites in Glacier Bay, Alaska, and noted a shift from positive to negative temperature growth response over the instrumental era (1832–1877, 1900–1993). Similarly, Campbell *et al.* (2021) found a range of climate responses for yellow-cedar depending on location and tree size. Much of the focus of yellow-cedar research has instead been on the recent decline of stands in southeastern Alaska and coastal British Columbia (*e.g.* Beier *et al.* 2008; Hennon *et al.* 2012; Barrett and Pattison 2017; Bidlack *et al.* 2017; Comeau *et al.* 2021; Gaglioti *et al.* 2021). However, this decline has been linked more strongly to a lack of insulating snow cover caused by warming temperatures rather than directly to temperature itself (Hennon *et al.* 2006, 2016). Those same dynamics and yellow-cedar decline do not appear to be present in the North Cascades.

Here, we evaluate whether it is possible to develop a temperature-sensitive tree-ring proxy record on the western slopes of the North Cascades to reconstruct regional summer temperatures over the last 500 years using three yellow-cedar chronologies from sites at Canyon Lake, Grouse Butte and Mount Pilchuck. In addition to traditional empirical statistical evaluation of the climate signal recorded by this species at these sites (Hughes 2011), we use a proxy system model (Vaganov *et al.* 2006; Evans *et al.* 2013) of tree-ring formation to explore whether growth variation can be mechanistically linked to temperature.

## DATA AND METHODS

### Site Description

Our three study sites are in mid-elevation montane forests on the mesic western slopes of the northern Cascade Mountains in Washington State (Figure 1; Table 1). The sites are in the mixed conifer zone with yellow-cedar co-dominant with other species including mountain hemlock and Pacific silver fir. Regional weather patterns are dominated by the Pacific maritime climate, typified by cool, moist winters and a generally dry growing season, with winter precipitation predominantly falling as snow above 1000 m a.s.l. (Franklin and Dyrness 1973). Minimum site temperatures are below freezing from mid-November through mid-April, and generally don't reach 5°C until June. Annual precipitation exceeds 260 cm at each site, with more than 80% falling outside the growing season, between

**Table 1.** Coordinates and topographic position of each of the three study sites. Data from Robertson (2011).

| Site | Latitude | Longitude | Aspect | Elevation (m) |
|---|---|---|---|---|
| Canyon Lake | 48.8119 | −122.0361 | NNW | 1310–1402 |
| Grouse Butte | 48.8150 | −121.9281 | NNE | 1219–1341 |
| Mount Pilchuck | 48.0708 | −121.8103 | N | 944–1005 |

October and May (Daly *et al.* 1994). The sites are steep with rocky and well-drained soils.

These sites were chosen for the presence of yellow-cedar growing in stands with exceptional ages. As far as we can tell, these yellow-cedar sites were not logged, or selectively logged, probably because they are typically on slopes that are too high, steep and rocky to have been economically worthwhile (Agee and Vaughn 1993). The fire-return interval here is typically in excess of 1000 years, which allows the establishment of old-growth stands like these (Franklin and Hemstrom 1981; LANDFIRE 2014). The most recent stand-replacing fire at the Canyon Lake site was likely around 1170 CE, and the predominant disturbance type at the site results from wind events.

## Sample Collection and Chronology Development

We took increment cores from living canopy dominant trees at each site (Table 2). All samples were prepared using standard techniques (Stokes and Smiley 1968; Cook and Kairiukstis 1990). Trees were selected for their position in the canopy structure, with care taken to ensure that no trees with visible damage were selected. Two cores were taken per tree when feasible, and the cores were air-dried, mounted, and sanded with increasingly finer grit sandpaper so that individual cells within each ring were clearly visible. We used a Velmex sliding stage to measure ring widths to the nearest 0.001 mm, and crossdated them visually and statistically (Bunn 2010).

To maintain low-frequency variation while removing age-specific growth patterns, we detrended each series using a modified negative exponential growth curve or straight line when the slope was greater than zero (Fritts *et al.* 1969), although age-dependent splines produced very similar results (Melvin *et al.* 2007). We used the bi-weight robust mean to estimate the mean chronology for each site, after truncating the chronologies when the sample depth dropped below five and when the subsample signal strength (SSS) dropped below 0.85 (Buras 2017). We also calculated a chronology using the first principal component (PC) from the three centered and scaled chronologies from each site. The choice to use the first PC is somewhat arbitrary as PC1 is essentially identical to a chronology composed of the yearly means of each site ($r > 0.99$). Summary statistics, including the mean interseries correlation ($\bar{r}$), EPS, SSS, were calculated for each of the chronologies. The interseries correlation was calculated by removing each core from the chronology and correlating it to the remaining chronology over the common interval. Expressed population signal and subsample signal strength are both measures of the strength of a common signal, with EPS used as an estimate of the true population and SSS representing the robustness of a chronology going back in time (Buras 2017).

**Table 2.** Select chronology statistics for sites. Though two cores were collected from each tree sampled, not all cores were usable. The average series length is given by $\bar{n}$, the time span shows the length of coverage at a site by at least one tree core. Also included are the mean interseries correlation ($\bar{r}$), mean first-order autocorrelation ($\bar{\phi}_1$, and the EPS of the chronology. The final chronology from Canyon Lake spanned 1290–2015, Grouse Butte 1333–2015, and Mount Pilchuck 1220–2015.

| Site | Trees | Cores | $\bar{n}$ | Start | End | $\bar{r}$ | $\bar{\phi}_1$ | EPS |
|---|---|---|---|---|---|---|---|---|
| Canyon Lake | 28 | 50 | 503 | 1221 | 2015 | 0.64 | 0.81 | 0.94 |
| Grouse Butte | 21 | 37 | 519 | 1067 | 2015 | 0.56 | 0.83 | 0.88 |
| Mount Pilchuck | 27 | 53 | 589 | 1075 | 2015 | 0.57 | 0.87 | 0.94 |

## Climate Data

We used output from the Variable Infiltration Capacity (VIC) hydrologic model to calculate various physiologically relevant influences on tree growth (Liang *et al.* 1994). The VIC model is a multiple soil-level model developed to couple the output of general circulation models to finer-scale local hydrological processes. Here we used a model simulation created by the Climate Impacts Group for the original purpose of modeling future regional streamflow conditions (Hamlet *et al.* 2012). The input data are 1/16$^{th}$ degree resolution (*ca.* 6 km) at daily resolution from 1915 to 2006 and run in the Columbia River and adjacent Puget Sound basins, calibrated to Columbia River main stem and tributary stream flow. Temperatures for the input data were derived from a network of regional meteorological COOP station data and interpolated over an elevation model. Output was calibrated to streamflow using station data primarily along the Columbia River and associated tributaries. Details on these data are summarized by Littell *et al.* (2016).

In addition to the VIC data, which includes physiologically useful metrics like snow water equivalent (SWE) and potential evapotranspiration (PET), we also used the 1/24$^{th}$ degree resolution (*ca.* 4km) PRISM data at monthly resolution over the time period 1895 to 2015 (Daly *et al.* 2002) in order to get a longer time-series of temperature and precipitation data for correlating against the tree-ring data. For potential evapotranspiration we used the "PET1" product that uses predefined vegetation classes and assumes that plant evapotranspiration is not limited by water supply as described in Littell *et al.* (2010). The PRISM data have been successfully used in many studies of tree growth and climate in areas of complex terrain (*e.g.* Salzer *et al.* 2009; Williams *et al.* 2010; Biondi *et al.* 2014; Evans *et al.* 2017). For the Vaganov-Shashkin modeling described in Section 3.5, we used the daily PRISM product from 1981 to 2015 in addition to the VIC data to evaluate model sensitivity to the choice of input data.

## Statistical Analysis

We aggregated the daily VIC data into monthly variables for each grid cell that corresponded to a site location. To evaluate possible energy- and temperature-limited associations, we use the average minimum and maximum daily temperatures, along with monthly mean snow water equivalent (SWE). Mean soil moisture and total monthly precipitation were used as metrics for water stress, and we also looked at growing season evapotranspiration deficit (ET Def), which is the difference between actual and potential evapotranspiration (PET-AET) (Stephenson 1998; Littell *et al.* 2008). We ran a bootstrapped monthly climate correlation analysis, using climate data form the previous year's growing season (py-May) through the end of the current year growing season (cy-September) compared against yearly growth (Biondi and Waikul 2004). Given the tendency for growth to be correlated with more than one climate variable we also looked at bootstrapped partial correlation analysis for selected variables. To assess statistical sensitivity to the choice of climate data, we also ran all analyses using the monthly values from PRISM.

## Forward Modeling

To complement the empirical statistical analysis described above, we also used the Vaganov-Shashkin forward model of tree-ring formation (VSM) to help understand the patterns seen in the yellow-cedar chronologies (Vaganov *et al.* 2006, 2011; Anchukaitis *et al.* 2020). Vaganov-Shashkin is a process-based proxy system model that uses piecewise linear functions of daylength, temperature, and soil moisture to estimate daily xylogenesis rates from limiting climatic factors and thus simulate the formation of annual tree rings as a function of climate. The model can reproduce tree-ring patterns across a wide range of species with different limiting factors (Vaganov *et al.* 1999, 2006, 2011; Anchukaitis *et al.* 2006, 2012, 2020; Evans *et al.* 2006; Shi *et al.* 2008; Bunn *et al.* 2018). We ran VSM using daily temperature and precipitation data over the period 1981 to 2015 from the PRISM model as well as the VIC data. Using VSM we were able to generate estimates of climate-limited annual growth as well as daily-scale information on the most limiting climatic factor from the simulation.

### Temperature Reconstruction

We used the leading principal component of our three chronologies (the "PC1 chronology") and the monthly PRISM climate data to calibrate a regression model of tree growth and mean summer temperature (June through August). We cross-validated the model using a 10-fold cross-validation process, whereby we randomly divided the data into ten-year segments in order to preserve the autocorrelation structure and trained ten models, each one withholding one of the segments. For each model run, we calculated the reduction of error (RE), coefficient of efficiency (CE), mean squared error (MSE), and coefficient of determination ($R^2$) of the calibration period, and calculated the median of each value as a measure of overall model skill. Reduction of error is a ratio of the error in the validation period to the error as compared to the mean during the calibration period, and the coefficient of efficiency is the error in the validation as compared to the mean during the validation period (Cook and Kairiukstis 1990; Cook *et al.* 1999). Values above zero suggest that the model does better than a random expectation in predicting the target. We ran this process 1000 times, and took the median of each model run. We analyzed the model residuals for their autocorrelation structure and applied a Breusch-Pagan test for heteroskedasticity. For comparison to the existing spatial NTREND temperature reconstruction, we extracted the temperature estimates from the nearest gridpoint to our sites from the reconstruction by Anchukaitis *et al.* (2017).

### Software

Our analysis relied heavily on the open-source software R version 4.1 (R Core Team 2021) and the associated packages dplR (Bunn 2008) and treeclim (Zang and Biondi 2015). Maps were created using QGIS software (QGIS Development Team 2018). The VSM model runs in MATLAB with code described in Anchukaitis *et al.* (2020).

## RESULTS

### Tree-Ring Chronologies

We built tree-ring chronologies from three sites with over 20 trees in each chronology and average segment length of over 500 years (Table 2). The oldest cores date back prior to 1100 CE at the Mount Pilchuck site and Grouse Butte. The chronologies all show good interseries correlation, high first-order autocorrelation, and a strong shared signal within each site (Table 2). The mean site chronologies for the yellow-cedar are each more than 750 years in length, with an adequate common signal back to 1333 CE (Figure 2).

We did not formally quantify frost rings in the cores. However, we observed very few frost rings in the cores prior to the 20$^{th}$ Century and only a handful after that. There was no clear coherency among or between sites in terms of frost-ring frequency.

### Climate–Growth Analysis

We observe a positive relationship with Yellow-cedar ring width and growing-season and previous-year minimum temperatures at each of the sites, and an inverse relationship with winter snowpack – especially at Canyon Lake (Figure 3). None of the chronologies showed a consistent seasonal sensitivity to precipitation. Weak relationships with winter maximum temperatures and evapotranspiration deficit exist but these are not consistent across sites. As expected, the first PC of the yellow-cedar chronologies showed similar sensitivities in terms of sign and magnitude. Correlations between tree growth and the PRISM temperature and precipitation data are similar and are not shown here.

A partial correlation analysis between tree growth, summer minimum temperatures, and spring SWE shows that temperature continues to be correlated with growth when first controlling for the effect of SWE for all the site chronologies and the PC1 chronology (Table 3). However, with the exception of Canyon Lake, the confidence intervals span zero in the correlations between growth and spring SWE when first controlling for temperature. These results are similar using VIC or PRISM as the climate data. We used Kendall's $\tau$ for the correlation, but other correlation measures (Pearson's $r$, and Spearman's $\rho$) also gave similar results.

### Forward Modeling

The results from the VSM process model supported the correlation analysis with both the daily

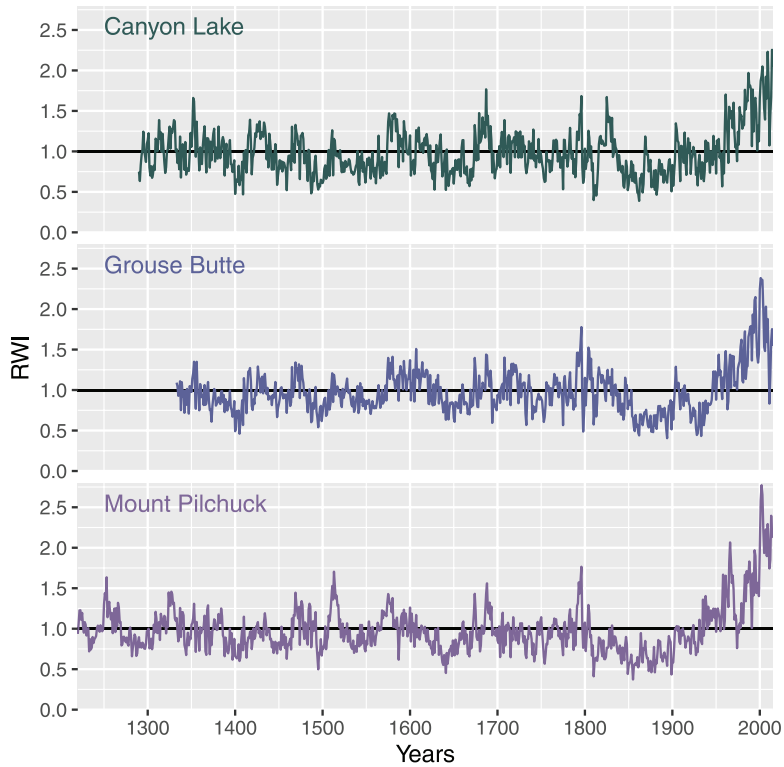


**Figure 2.** Mean-value tree-ring width chronologies for each site.

VIC and the daily PRISM data used as drivers. The results are broadly similar whether using the PRISM or the VIC daily data. VSM captures interannual variation at two of the sites and composite chronology with reasonable skill (Canyon Lake $r = 0.42$, Grouse Butte $r = 0.40$, PC1 $r = 0.48$). Growth at the Mt Pilchuck site was not skillfully simulated ($r = 0.19$), however, which may simply reflect the site chronology's relatively poor correlation to the instrumental climate data compared to the other sites. The model simulations of the PC1 chronology show that growth was directly limited by temperature through most of the growing season (Figure 4), with energy limitation and soil moisture playing secondary and more limited roles. This pattern is observed for the individual sites as well (not shown).

**Table 3.** Partial correlations analysis for growth and climate using Kendall's $\tau$. Bootstrapped 95% confidence intervals are shown in parentheses. $\tau_{RW,Tmin|SWE}$ shows the correlation between ring width and summer minimum temperatures while controlling for spring SWE, and $\tau_{RW,SWE|Tmin}$ shows the correlation between ring width and spring SWE while controlling for summer minimum temperatures. Bolded values show correlations where the confidence intervals do not span zero.

| Site | $\tau_{RW,SWE\|Tmin}$ | $\tau_{RW,Tmin\|SWE}$ |
|---|---|---|
| Canyon Lake | **−0.19 (−0.29, −0.07)** | **0.33 (0.23, 0.43)** |
| Grouse Butte | −0.07 (−0.18, 0.06) | **0.26 (0.13, 0.38)** |
| Mount Pilchuck | −0.03 (−0.15, 0.09) | **0.46 (0.35, 0.55)** |
| First PC | −0.1 (−0.2, 0.02) | **0.42 (0.32, 0.51)** |

## Temperature Reconstruction

The temperature reconstruction of minimum summer temperatures using PC1 covers the period 1333–2015 CE and shows a relatively cold 19th Century and a characteristic warming trend in temperatures in the latter half of the 20th Century (Figure 5). The reconstructed temperatures prior to the 19th Century show considerable decadal variability and during their period of overlap capture the variability observed in the instrumental data. The

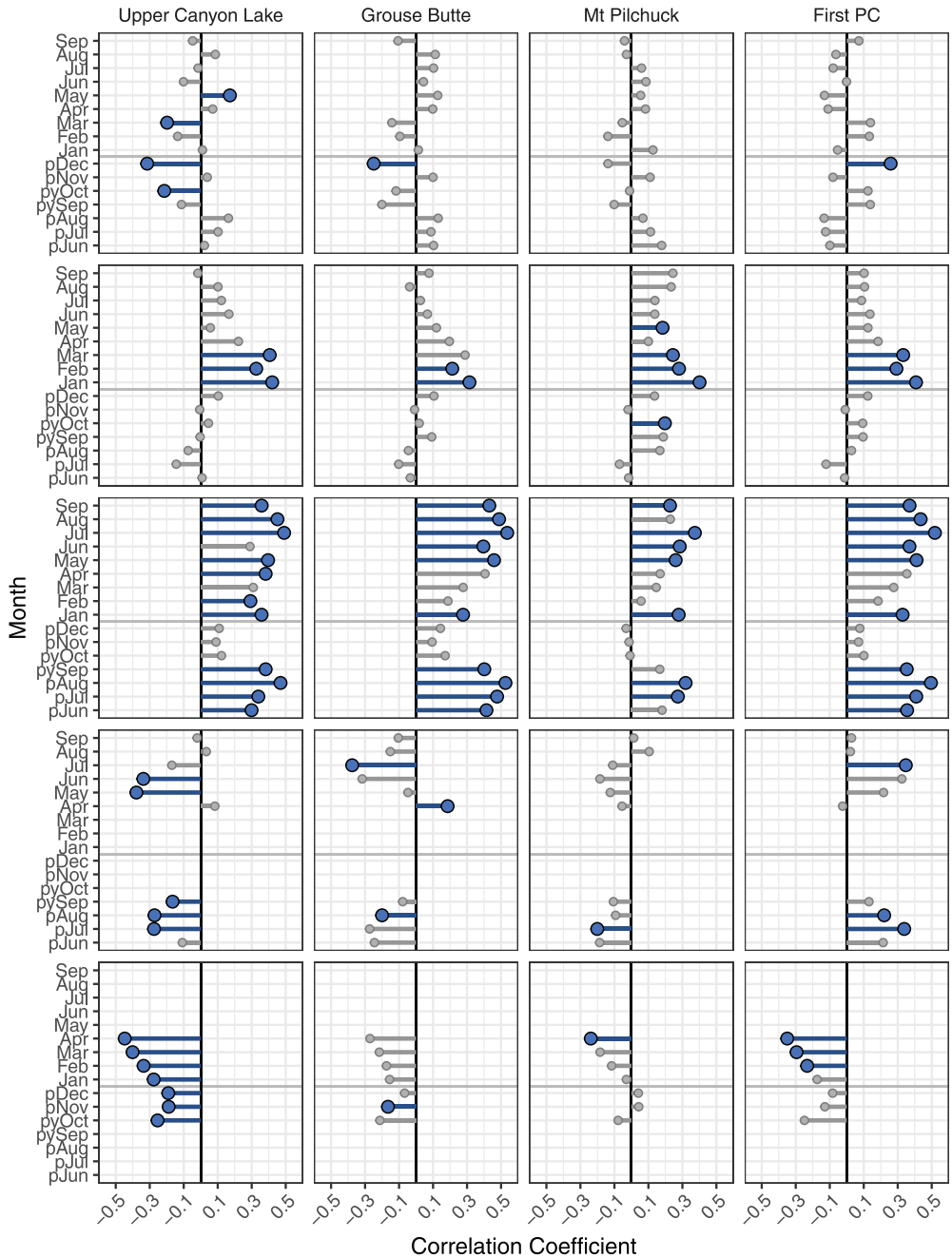


**Figure 3.** Monthly bootstrapped climate correlations between each of the chronologies and monthly climate variables from the VIC model. Monthly climate variables shown are total precipitation, average daily maximum and minimum temperatures, total monthly evapotranspiration deficit (ET Def), and first-of-the-month snow water equivalent (SWE). Bootstrapped monthly climate correlations are calculated for each month from June of the previous year through September of the current year, compared against each year of tree growth. Direction and strength of all correlations are shown, with the non-significant ($p > 0.05$) correlations in (light) grey.

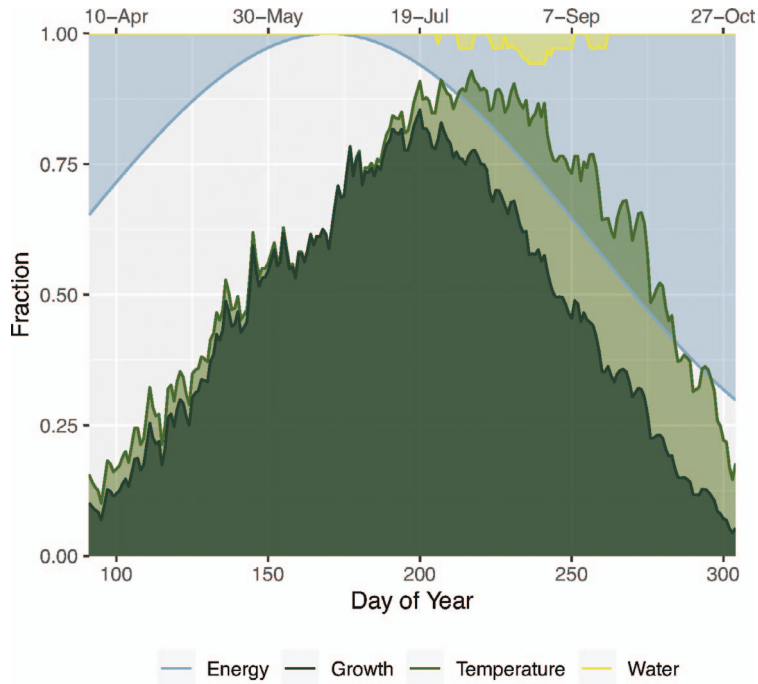


**Figure 4.** Average limiting factors on growth from the Vaganov-Shashkin model simulated from 1981 to 2015. The model calculates growth limitations on a relative scale (0 to 1, y-axis) and the simulated cambial growth on any given day (x-axis) is therefore controlled by the most limiting factor (temperature, energy, or water).

cross-validated skill diagnostics suggest an adequate reconstruction ($r^2 = 0.44$, CE = 0.35, RE = 0.32, MSE = 0.59). Residuals were homoskedastic and showed no significant autocorrelation.

Although our reconstruction compares favorably with the NTREND reconstruction over the 20th Century ($r = 0.41$ interannual, $r = 0.76$ at decadal), there are substantial differences prior to

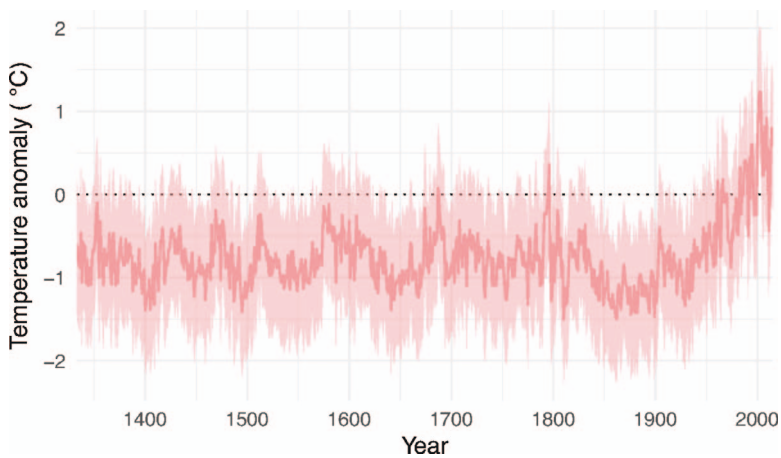


**Figure 5.** Reconstructed minimum summer temperature anomalies compared to the 1961–1990 climate normal. This reconstruction is derived from the first principal component of the three yellow-cedar site chronologies ('PC1 chronology'), and the instrumental temperature target is the mean minimum summer (June through August) temperature. The error envelope is 2 times the model MSE of the reconstruction.

the instrumental period (Figure 6). The regional NTREND reconstruction correlates with our PC1 reconstruction at $r = 0.26$ interannually and at $r = 0.43$ at decadal scales over the entire period. The NTREND reconstruction also correlates weakly with the local PRISM data at $r = 0.13$ and at $r = 0.54$ at decadal time scales. Indeed, in the NTREND spatial reconstruction our region shows relatively poor validation skill (Anchukaitis *et al.* 2017).

## DISCUSSION

Our results demonstrate that high elevation yellow-cedar in the Pacific Northwest have many qualities that make these trees well suited for dendroclimatology, including a strong common signal, long segment lengths, and broad geographical distribution (Cook and Kairiukstis 1990). Both statistical and forward modeling suggest that temperature is the primary limiting factor to growth over the period analyzed, which would make this species one of the relatively few long-lived tree-ring temperature proxies in the continental United States.

Although tree rings from yellow-cedar have been used in a variety of other applications, we believe that they can be successfully used for reconstructing temperature if the trees sampled are from sufficiently high-elevation sites. The trees in our study were growing at 900–1400 meters a.s.l. and were sampled opportunistically to find long-lived trees at the highest elevations possible. In the course of this work, we identified potential additional sites with yellow-cedar growing at elevations $>$ 2000 m in the Washington Cascades. However, we could not find stands of long-lived trees at these higher elevation locations. Because the diameter of the trees at breast height in this work often exceeded 2 m, we were also not able to extract the entire record from the trees we sampled and were unable in many cases to reach the pith. The challenge for future work will be to locate and collect from sites that are at both high elevation and contain older yellow-cedar with long segment lengths. Part of that work will involve determining the appropriate elevation range as well as possible topoclimatic settings for robust reconstructions. Work by Bunn *et al.* (2018) showed that even minor changes in elevation, slope, and aspect can affect local temperature and confound the climate–growth signal in areas of complex terrain. The weaker correlation of growth and climate at the Mt Pilchuck site as compared to the other two sites might be an artifact of its relatively low elevation as well as its topographic setting.

### Limitations to Climate–Growth Analysis

An interesting aspect of the correlation analysis shown in Figure 3 is the association between tree growth and summer minimum temperatures. It's also interesting that there are strong negative correlations between growth and SWE during the late winter and early spring months especially at Canyon Lake and in the chronology from the first principal component. To begin to disentangle these two correlates we used a partial correlation analysis to look at the association between growth and temperature while controlling for SWE and vice versa. This showed that the temperature correlation remains robust while considering SWE, but that the opposite is not generally true (Table 3). This test supports our conclusion that it is temperature, rather than the direct influence of snow, that is the primary control on yellow-cedar growth at these sites.

It remains a perennial challenge to robustly establish a true temperature limitation on tree growth when both water stress and snowpack can contribute to tree growth variability. In this study, we attempted to account for and minimize the potential for multiple limiting factors to confound a clear interpretation of growth limitation. First, we used climate data informed by the VIC model, which included more relevant variables such as SWE and evapotranspiration deficit (Figure 3). We also used a process model to explicitly model growth using water and energy limitation (Figure 4). Both of these analyses supported our finding that temperature is the primary limiting factor for these high elevation yellow-cedar chronologies. Finally, our interpretation of the partial correlation analysis including SWE and temperature (Table 3) is that temperature is the primary limiting factor and that SWE at these sites responds to temperature but is not the primary control on tree growth.

Although our analyses do support a direct temperature limitation in these high-elevation yellow-cedar, we note several observations that are

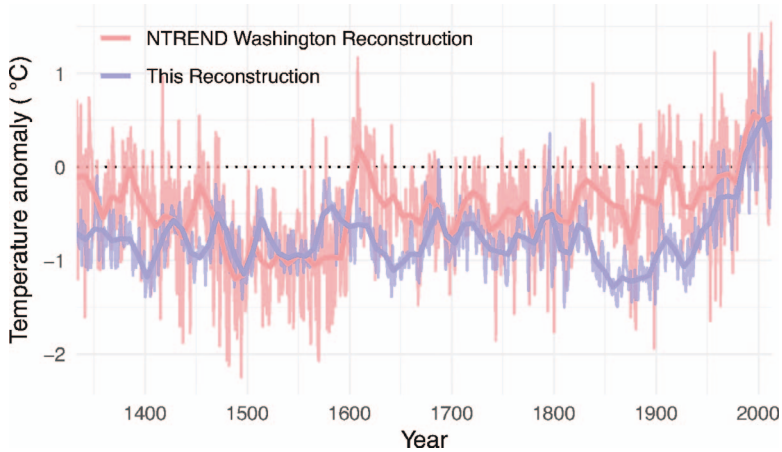


**Figure 6.** The temperature reconstruction developed in this study compared against the corresponding gridded NTREND spatial reconstruction (Anchukaitis *et al.* 2017) grid point for our study region. Temperatures are shown as departure from the 1961–1990 climate normal. Also shown is a loess smooth with a 10-year span for each reconstruction to highlight decadal variability.

thus far unexplained. As we previously noted, a curious aspect of our study is that we found average daily minimum temperatures were the strongest correlate to ring width. We cannot explain why tree growth would be most strongly associated with minimum temperatures rather than average or maximum temperatures. It is possible in these settings that the complex terrain of the North Cascades leads to cold air pooling that dominates the local temperature profile. However, we would need longer-term site-specific meteorological monitoring to address the roles that minimum temperatures vs. maximum temperatures have in shaping the daily temperature profile. The minimum temperature response does not, however, appear to be associated with differential trends in the temperature variables, as the observed relationships largely persist when the climate data are detrended prior to analysis.

## Comparison to NTREND

We do not know the precise reason for the disagreement between the local grid point NTREND reconstruction and our new reconstruction using yellow-cedar (Figure 6). Although NTREND compares moderately well to our reconstruction in the 20$^{th}$ Century, the reconstructions disagree with one another prior to that recent period. It is possible that temperatures trends and anomalies in the Washington Cascades and at hemispheric scales have greater spatiotemporal similarity in the 20$^{th}$ Century but less prior to the period of rapid anthropogenic warming. This aspect of spatial fingerprinting is common in situations where internal dynamics can cause either widespread or localized differences in climate such as with the expression of the Medieval Climatic Anomaly and the Little Ice Age, which differ from modern forcing that is driven by anthropogenic forcing (Bradley *et al.* 2003; Osborn and Briffa 2006; Goosse *et al.* 2012). Another notable difference between this reconstruction and the NTREND reconstruction is a reduced interannual variability in the reconstructed temperatures from yellow-cedar. Ecologically, this could be attributed to the moderating influence of marine air that is not captured by the continental chronologies used by NTREND or by our climate data. Alternatively, this may simply reflect the difference in both climate targets and statistical methodologies in Anchukaitis *et al.* (2017) and the current study. NTREND for instance targets the relatively coarse Kriged version of HadCRUT4 (Cowtan and Way 2014), in contrast to the high spatial resolution gridded climate data used here. Finally, the NTREND reconstruction skill is comparatively low in the co-located grid point to our current study, and it may simply be that the long distances between the climate conditions in

this region and the information available from more distal and interior tree-ring chronologies results in an NTREND reconstruction that is less representative at the local scales considered here.

### Recent Temperature Trends and Comparison to Other Studies

The anomalous temperatures seen in the 20th Century of this reconstruction are consistent with a host of similar studies that put recent warming into a long-term context and summarized by Wilson *et al.* (2016) and Esper *et al.* (2018). Our reconstruction, although preliminary, suggests that recent temperatures in the North Cascades are likely unprecedented for at least the past six centuries.

The most comprehensive tree-ring study of regional temperatures comes from Graumlich and Brubaker (1986). In that study the authors used mountain hemlock and subalpine larch in a novel response-surface analysis framework to reconstruct mean annual temperature. Their results are similar to ours in showing that preindustrial temperatures were *ca*. 1°C lower than the recent modern period. The Graumlich and Brubaker (1986) study was also notable as an early effort to unmix confounding signals of snowpack and temperatures using a multispecies composite for the reconstruction. Like Graumlich and Brubaker (1986), our reconstruction shows high temperature anomalies at the end of the record, but does not show evidence of declining tree growth after *ca*. 1950.

The lack of consistent or commonly shared frost rings is notable. One might expect that trees sensitive to minimum temperatures and SWE would be prone to the formation of frost rings. An avenue of research that could shed light on this would be the application of staining to look for partial lignification that has been associated with frost events (Piermattei *et al.* 2020; Tardif *et al.* 2020). It is possible that the qualitatively observed increased frequency of frost rings in the 20th Century could be consistent with the dieback research that has been clearly shown in other studies of yellow-cedar (*e.g.* Beier *et al.* 2008; Hennon *et al.* 2012, 2016; Barrett and Pattison 2017; Bidlack *et al.* 2017; Comeau *et al.* 2021; Gaglioti *et al.* 2021).

## SUMMARY AND PROSPECTUS

Based on our findings, we believe that yellow-cedar at high elevations in the Pacific Northwest shows potential for use in proxy temperature reconstructions. The species has not previously been a focus of climate sensitivity studies at these elevations and our work now provides evidence of its utility in understanding past temperatures. With expanded sampling efforts guided by our findings, we are confident that this species can yield a record of at least one thousand years and therefore contribute to large-scale temperature reconstructions. This species also occurs in isolated pockets at high elevations as far south as 41.6°N in the Klamath National Forest in northern California and further west (*ca*. 123.5°W) in the Olympic Peninsula (Murray 2010). We believe that a broader sampling across this range could significantly improve our understanding of past climate variability in this region of North America. Expanding the spatial extent of yellow-cedar chronologies would also allow for spatial field reconstructions that were explored in Trinies (2019).

It is also likely that measuring additional proxies, including both quantitative wood anatomy (Lange *et al.* 2020; Edwards *et al.* 2021) and blue intensity (Wilson *et al.* 2017; Wiles *et al.* 2019; Wilson *et al.* 2019; Heeter *et al.* 2021), could further provide useful temperature information and disentangle any competing climate signals from this species and region.

## ACKNOWLEDGMENTS AND DATA AVAILABILITY

We thank the three anonymous reviewers whose comments and suggestions helped improve and clarify this manuscript. CAT was partially supported with funds from the WWU Graduate School. KJA was partially supported by grants from the US National Science Foundation (BCS-1759629 and AGS-1803995) for this project.

The tree-ring data in this paper are available on the International Tree-Ring Data Bank.

## REFERENCES CITED

Agee, J. K., and M. Vaughn, 1993. *The Headwaters Old Growth of Canyon Lake Creek. Technical report*, Trillium Corporation and Whatcom Community Land Trust, Bellingham.

Anchukaitis, K. J., P. Breitenmoser, K. R. Briffa, A. Buchwal, U. Büntgen, E. R. Cook, R. D. D'Arrigo, J. Esper, M. N. Evans, D. Frank, H. Grudd, B. E. Gunnarson, M. K. Hughes, A. V. Kirdyanov, C. Körner, P. J. Krusic, B. Luckman, T. M. Melvin, M. W. Salzer, A. V. Shashkin, C. Timmreck, E. A. Vaganov, and R. J. S. Wilson, 2012. Tree rings and volcanic cooling. *Nature Geoscience* 5:836–837.

Anchukaitis, K. J., M. N. Evans, M. K. Hughes, and E. A. Vaganov, 2020. An interpreted language implementation of the Vaganov–Shashkin tree-ring proxy system model. *Dendrochronologia* 60:125677. https://doi.org/10.1016/j.dendro.2020.125677.

Anchukaitis, K. J., 2017. Tree rings reveal climate change past, present, and future. *Proceeding of the American Philosophical Society* 161:244–263.

Anchukaitis, K. J., M. N. Evans, A. Kaplan, E. A. Vaganov, M. K. Hughes, H. D. Grissino-Mayer, and M. A. Cane, 2006. Forward modeling of regional scale tree-ring patterns in the southeastern United States and the recent influence of summer drought. *Geophysical Research Letters* 33. https://doi.org/10.1029/2005GL025050.

Anchukaitis, K. J., R. J. S. Wilson, K. R. Briffa, U. Büntgen, E. R. Cook, R. D. D'Arrigo, N. Davi, J. Esper, D. C. Frank, B. E. Gunnarson, G. C. Hegerl, S. Helama, S. Klesse, P. J. Krusic, H. W. Linderholm, V. Myglan, T. J. Osborn, P. Zhang, M. Rydval, L. Schneider, A. Schurer, G. C. Wiles, and E. Zorita, 2017. Last millennium Northern Hemisphere summer temperatures from tree rings: Part II, Spatially resolved reconstructions. *Quaternary Science Reviews* 163:1–22.

Ault, T., C. Deser, M. Newman, and J. Emile-Geay, 2013. Characterizing decadal to centennial variability in the equatorial Pacific during the last millennium. *Geophysical Research Letters* 40:3450–3456.

Barrett, T. M., and R. R. Pattison, 2017. No evidence of recent (1995–2013) decrease of yellow-cedar in Alaska. *Canadian Journal of Forest Research* 47:97–105.

Beier, C. M., S. E. Sink, P. E. Hennon, D. V. D'Amore, and G. P. Juday, 2008. Twentieth-century warming and the dendroclimatology of declining yellow-cedar forests in southeastern Alaska. *Canadian Journal of Forest Research* 38: 1319–1334.

Bidlack, A., S. Bisbing, B. Buma, D. V. D'Amore, P. E. Hennon, T. Heutte, J. Krapek, R. Mulvey, and L. Oakes, 2017. Alternative interpretation and scale-based context for "No evidence of recent (1995–2013) decrease of yellow-cedar in Alaska" (Barrett and Pattison 2017). *Canadian Journal of Forest Research* 47:1145–1151.

Biondi, F., M. Hay, and S. Strachan, 2014. The tree-ring interpolation model (TRIM) and its application to *Pinus monophylla* chronologies in the Great Basin of North America. *Forestry* 87:582–597.

Biondi, F., and K. Waikul, 2004. DENDROCLIM2002: A C++ program for statistical calibration of climate signals in tree-ring chronologies. *Computers and Geosciences* 30:303–311.

Bradley, R. S., M. K. Hughes, and H. F. Diaz, 2003. Climate in medieval time. *Science* 302:404–405.

Briffa, K., and P. Jones, 1993. Global surface air temperature variations during the twentieth century: Part 2, Implications for large-scale high-frequency palaeoclimatic studies. *The Holocene* 3:77–88.

Brubaker, L. B., 1980. Spatial patterns of tree growth anomalies in the Pacific Northwest. *Ecology* 61:798–807.

Bunn, A. G., 2008. A dendrochronology program library in R (dplR). *Dendrochronologia* 26:115–124.

Bunn, A. G., 2010. Statistical and visual crossdating in R using the dplR library. *Dendrochronologia* 28:251–258.

Bunn, A. G., M. W. Salzer, K. J. Anchukaitis, J. M. Bruening, and M. K. Hughes, 2018. Spatiotemporal variability in the climate growth response of high elevation bristlecone pine in the White Mountains of California. *Geophysical Research Letters* 45:13312–13321.

Buras, A., 2017. A comment on the expressed population signal. *Dendrochronologia* 44:130–132.

Campbell, E. M., S. Magnussen, J. A. Antos, and R. Parish, 2021. Size-, species-, and site-specific tree growth responses to climate variability in old-growth subalpine forests. *Ecosphere* 12:e03529. https://doi.org/10.1002/ecs2.3529.

Case, M. J., and D. L. Peterson, 2007. Growth-climate relations of lodgepole pine in the North Cascades National Park, Washington. *Northwest Science* 81:62–75.

Coats, S., J. E. Smerdon, B. I. Cook, R. Seager, E. R. Cook, and K. J. Anchukaitis, 2016. Internal ocean-atmosphere variability drives megadroughts in Western North America. *Geophysical Research Letters* 43:9886–9894.

Cobb, K. M., N. Westphal, H. R. Sayani, J. T. Watson, E. Di Lorenzo, H. Cheng, R. Edwards, and C. D. Charles, 2013. Highly variable El Niño–Southern Oscillation throughout the Holocene. *Science* 339:67–70.

Comeau, V. M., L. D. Daniels, and S. Zeglen, 2021. Climate-induced yellow-cedar decline on the island archipelago of Haida Gwaii. *Ecosphere* 12. DOI:10.1002/ecs2.3427.

Consortium, P. H., 2017. Comparing proxy and model estimates of hydroclimate variability and change over the Common Era. *Climate of the Past* 13:1851–1900.

Cook, E. R., and L. A. Kairiukstis, Editors, 1990. *Methods of Dendrochronology: Applications in the Environmental Science*. Kluwer Academic Publishers, Dordrecht.

Cook, E. R., D. M. Meko, D. W. Stahle, and M. K. Cleaveland, 1999. Drought reconstructions for the continental United States. *Journal of Climate* 12:1145–1162.

Coulthard, B. L., K. J. Anchukaitis, G. T. Pederson, E. Cook, J. Littell, and D. J. Smith, 2021. Snowpack signals in North American tree rings. *Environmental Research Letters* 16:034037. https://doi.org/10.1088/1748-9326/abd5de.

Cowtan, K., and R. G. Way, 2014. Coverage bias in the HadCRUT4 temperature series and its impact on recent temperature trends. *Quarterly Journal of the Royal Meteorological Society* 140:1935–1944.

Daly, C., W. P. Gibson, G. H. Taylor, G. L. Johnson, and P. P. Pasteris, 2002. A knowledge-based approach to the statistical mapping of climate. *Climate Research* 22: 99–113.

Daly, C., R. P. Neilson, and D. L. Phillips, 1994. A statistical-topographic model for mapping climatological precipitation over mountainous terrain. *Journal of Applied Meteorology* 33:140–158.

Dannenberg, M. P., and E. K. Wise, 2016. Seasonal climate signals from multiple tree ring metrics: A case study of *Pinus ponderosa* in the upper Columbia River Basin. *Journal of Geophysical Research: Biogeosciences* 121:1178–1189.

Edwards, J., K. J. Anchukaitis, B. Zambri, L. Andreu-Hayles, R. Oelkers, R. D'Arrigo, and G. von Arx, 2021. Intra-annual climate anomalies in northwestern North America following the 1783–1784 CE Laki Eruption. *Journal of Geophysical Research: Atmospheres* 126. https://doi.org/10.1029/2020JD033544.

Emile-Geay, J., K. M. Cobb, M. E. Mann, and A. T. Wittenberg, 2013. Estimating central equatorial Pacific SST variability over the past millennium. Part II: Reconstructions and implications. *Journal of Climate* 26:2329–2352.

Esper, J., S. S. George, K. Anchukaitis, R. D'Arrigo, F. C. Ljungqvist, J. Luterbacher, L. Schneider, M. Stoffel, R. Wilson, and U. Büntgen, 2018. Large-scale, millennial-length temperature reconstructions from tree-rings. *Dendrochronologia* 50:81–90.

Esper, J., P. J. Krusic, F. C. Ljungqvist, J. Luterbacher, M. Carrer, E. Cook, N. K. Davi, C. Hartl-Meier, A. Kirdyanov, O. Konter, V. Myglan, M. Timonen, K. Treydte, V. Trouet, R. Villalba, B. Yang, and U. Büntgen, 2016. Ranking of tree-ring based temperature reconstructions of the past millennium. *Quaternary Science Reviews* 145:134–151.

Evans, M. E. K., D. A. Falk, A. Arizpe, T. L. Swetnam, F. Babst, and K. E. Holsinger, 2017. Fusing tree-ring and forest inventory data to infer influences on tree growth. *Ecosphere* 8: 1–20.

Evans, M. N., B. K. Reichert, A. Kaplan, K. J. Anchukaitis, E. A. Vaganov, M. K. Hughes, and M. A. Cane, 2006. A forward modeling approach to paleoclimatic interpretation of tree-ring data. *Journal of Geophysical Research: Biogeosciences* 111. https://doi.org/10.1029/2006JG000166.

Evans, M. N., S. E. Tolwinski-Ward, D. M. Thompson, and K. J. Anchukaitis, 2013. Applications of proxy system modeling in high resolution paleoclimatology. *Quaternary science reviews* 76:16–28.

Franklin, J. F., and C. T. Dyrness, 1973. *Natural Vegetation of Oregon and Washington*. Technical Report PNW-8, Pacific Northwest Forest and Range Experiment Station, Corvallis, Oregon.

Franklin, J. F., and M. A. Hemstrom, 1981. Aspects of succession in the coniferous forests of the Pacific Northwest. In *Forest Succession*, edited by H. H. Shugart and D. B. Botkin, chapter 14, pp. 212–229. *Springer Advanced Textx in Life Sciences*, Springer, New York.

Fritts, H. C., 1966. Growth-rings of trees: Their correlation with climate. *Science* 154:973–979.

Fritts, H. C., J. E. Mosimann, and C. P. Bottorff, 1969. A revised computer program for standardizing tree-ring series. *Tree-Ring Bulletin* 29:15–20.

Gaglioti, B. V., D. H. Mann, G. Wiles, and N. Wiesenberg, 2021. Is the modern-day dieback of yellow-cedar unprecedented? *Canadian Journal of Forest Research* 51:1953–1965.

Goosse, H., E. Crespin, S. Dubinkina, M.-F. Loutre, M. E. Mann, H. Renssen, Y. Sallaz-Damaz, and D. Shindell, 2012. The role of forcing and internal dynamics in explaining the "medieval climate anomaly". *Climate Dynamics* 39: 2847–2866.

Graumlich, L. J., 1987. Precipitation variation in the Pacific Northwest (1675–1975) as reconstructed from tree rings. *Annals of the Association of American Geographers* 77:19–29.

Graumlich, L. J., and L. B. Brubaker, 1986. Reconstruction of annual temperature (1590–1979) for Longmire, Washington, derived from tree rings. *Quaternary Research* 25: 223–234.

Guillet, S., C. Corona, M. Stoffel, M. Khodri, F. Lavigne, P. Ortega, N. Eckert, P. D. Sielenou, V. Daux, O. V. Churakova (Sidorova), N. Davi, J.-L. Edouard, Y. Zhang, B. H. Luckman, V. S. Myglan, J. Guiot, M. Beniston, V. Masson-Delmotte, and C. Oppenheimer, 2017. Climate response to the Samalas volcanic eruption in 1257 revealed by proxy records. *Nature Geoscience* 10:123–128.

Hamlet, A. F., E. P. Salathé, and P. Carrasco, 2012. *Statistical Downscaling Techniques for Global Climate Model Simulations of Temperature and Precipitation with Application to Water Resources Planning Studies*. Technical Report 4, University of Washington, Seattle.

Harley, G. L., R. S. Maxwell, B. A. Black, and M. F. Bekker, 2020. A multi-century, tree-ring-derived perspective of the North Cascades (USA) 2014–2016 snow drought. *Climatic Change* 162:127–143.

Heeter, K. J., G. L. Harley, J. T. Maxwell, R. J. Wilson, J. T. Abatzoglou, S. A. Rayback, M. L. Rochner, and K. A. Kitchens, 2021. Summer temperature variability since 1730 CE across the low-to-mid latitudes of western North America from a tree ring blue intensity network. *Quaternary Science Reviews* 267:107064.

Hegerl, G. C., T. J. Crowley, W. T. Hyde, and D. J. Frame, 2006. Climate sensitivity constrained by temperature reconstructions over the past seven centuries. *Nature* 440:1029–1032.

Hennon, P. E., D. V. D'Amore, P. G. Schaberg, D. T. Wittwer, and C. S. Shanley, 2012. Shifting climate, altered niche, and a dynamic conservation strategy for yellow-cedar in the North Pacific Coastal Rainforest. *BioScience* 62:147–158.

Hennon, P. E., D. V. D'Amore, D. T. Wittwer, A. Johnson, P. G. Schaberg, G. J. Hawley, C. M. Beier, S. E. Sink, and G. P. Juday, 2006. Climate warming, reduced snow, and freezing injury could explain the demise of yellow-cedar in southeast Alaska, USA. *World Resource Review* 18: 427–450.

Hennon, P. E., C. M. McKenzie, D. V. D'Amore, D. T. Wittwer, R. Mulvey, M. S. Lamb, F. E. Biles, and R. C. Cronn, 2016. *A Climate Adaptation Strategy for Conservation and Management of Yellow-Cedar in Alaska*. Technical Report GTR-917, Pacific Northwest Research station, US Forest Service, Portland, Oregon.

Hernández, A., C. Martin-Puertas, P. Moffa-S´anchez, E. Moreno-Chamarro, P. Ortega, S. Blockley, K. M. Cobb, L. Comas-Bru, S. Giralt, H. Goosse, J. Luterbacher, B. Martrat, R. Muscheler, A. Parnell, S. Pla-Rabes, J. Sjolte, A. A. Scaife, D. Swingedouw, E. Wise, and G. Xu, 2020. Modes of climate variability: Synthesis and review of proxy-based reconstructions through the Holocene. *Earth-Science Reviews* 209. https://doi.org/10.1016/j.earscirev.2020.103286.

Hughes, M. K., 2011. Dendroclimatology in high-resolution paleoclimatology. In *Dendroclimatology: Progress and Prospects*, edited by M. K. Hughes, T. W. Swetnam, and H. F. Diaz, pp. 17–34, Springer, Netherlands, Dordrecht.

Jones, P. D., and K. R. Briffa, 1992. Global surface air temperature variations during the twentieth century: Part 1, Spatial, temporal and seasonal details. *The Holocene* 2: 165–179.

Kemp-Jennings, S., D. L. Peterson, and A. G. Bunn, 2021. Temporal variability in climate-growth response of Mountain Hemlock at treeline in Washington and Oregon. *Northwest Science* 94:286–301.

King, J. M., K. J. Anchukaitis, J. E. Tierney, G. J. Hakim, J. Emile-Geay, F. Zhu, and R. Wilson, 2021. A data assimilation approach to last millennium temperature field reconstruction using a limited high-sensitivity proxy network. *Journal of Climate* 34(17):7091–7111.

Körner, C., 2012. *Alpine Treelines*. Springer, Basel.

Kusnierczyk, E. R., and G. J. Ettl, 2002. Growth response of ponderosa pine (*Pinus ponderosa*) to climate in the eastern Cascade Mountains, Washington, U.S.A.: Implications for climatic change. *Ecoscience* 9:544–551.

LANDFIRE, 2014. *Mean Fire Return Interval Layer*. U.S. Department of Interior, Geological Survey, and U.S. Department of Agriculture. [Online]. Available at http://landfire.cr.usgs.gov/viewer/.

Lange, J., M. Carrer, M. F. Pisaric, T. J. Porter, J.-W. Seo, M. Trouillier, and M. Wilmking, 2020. Moisture-driven shift in the climate sensitivity of white spruce xylem anatomical traits is coupled to large-scale oscillation patterns across northern treeline in northwest North America. *Global Change Biology* 26:1842–1856.

Laroque, C. P., and D. J. Smith, 1999. Tree-ring analysis of yellow-cedar (*Chamaecyparis nootkatensis*) on Vancouver Island, British Columbia. *Canadian Journal of Forest Research* 29:115–123.

Liang, X., D. P. Lettenmaier, E. F. Wood, and S. J. Burges, 1994. A simple hydrologically based model of land surface water and energy fluxes for general circulation models. *Journal of Geophysical Research* 99:14415–14428.

Littell, J. S., E. E. Oneil, D. McKenzie, J. A. Hicke, J. A. Lutz, R. A. Norheim, and M. M. Elsner, 2010. Forest ecosystems, disturbance, and climatic change in Washington State, USA. *Climatic Change* 102:129–158.

Littell, J. S., G. T. Pederson, S. T. Gray, M. Tjoelker, A. F. Hamlet, and C. A. Woodhouse, 2016. Reconstructions of Columbia River streamflow from tree-ring chronologies in the Pacific Northwest, USA. *JAWRA Journal of the American Water Resources Association* 52(5):1121–1141. https://doi.org/10.1111/1752-1688.12442.

Littell, J. S., D. L. Peterson, and M. Tjoelker, 2008. Douglas-fir growth in mountain ecosystems: Water limits tree growth from stand to region. *Ecological Monographs* 78:349–368.

Martin, J. T., G. T. Pederson, C. A. Woodhouse, E. R. Cook, G. J. McCabe, K. J. Anchukaitis, E. K. Wise, P. J. Erger, L. Dolan, M. McGuire, S. Gangopadhyay, K. J. Chase, J. S. Littell, S. T. Gray, S. S. George, J. M. Friedman, D. J. Sauchyn, J.-M. St-Jacques, and J. King, 2020. Increased drought severity tracks warming in the United States' largest river basin. *Proceedings of the National Academy of Sciences* 117:11328–11336.

Melvin, T. M., K. R. Briffa, K. Nicolussi, and M. Grabner, 2007. Time-varying-response smoothing. *Dendrochronologia* 25: 65–69.

Murray, M. D., 2010. The natural range of yellow-cedar: A photographic tour of diverse locations. In *A Tale of Two Cedars – International Symposium on Western Redcedar and Yellow-Cedar*. General Technical Report PNW-GTR-828, pp. 149–152.

Osborn, T. J., and K. R. Briffa, 2006. The spatial extent of 20th-century warmth in the context of the past 1200 years. *Science* 311:841–844.

Peterson, D. W., and D. L. Peterson, 2001. Mountain hemlock growth responds to climatic variability at annual and decadal time scales. *Ecology* 82:3330–3345.

Peterson, D. W., D. L. Peterson, and G. J. Ettl, 2002. Growth responses of subalpine fir to climatic variability in the Pacific Northwest. *Canadian Journal of Forest Research* 32: 1503–1517.

Piermattei, A., A. Crivellaro, P. J. Krusic, J. Esper, P. Vítek, C. Oppenheimer, M. Felhofer, N. Gierlinger, F. Reinig, O. Urban, A. Verstege, H. Lobo, and U. Büntgen, 2020. A millennium-long 'Blue Ring' chronology from the Spanish Pyrenees reveals severe ephemeral summer cooling after volcanic eruptions. *Environmental Research Letters* 15:124016. https://doi.org/10.1088/1748-9326/abc120.

Power, S., M. Lengaigne, A. Capotondi, M. Khodri, J. Vialard, B. Jebri, E. Guilyardi, S. McGregor, J.-S. Kug, M. Newman, M. J. McPhaden, G. Meehl, D. Smith, J. Cole, J. Emile-Geay, D. Vimont, A. T. Wittenberg, M. Collins, G.-I. Kim, W. Cai, Y. Okumura, C. Chung, K. M. Cobb, F. Delage, Y. Y. Planton, A. Levine, F. Zhu, J. Sprintall, E. D. Lorenzo, X. Zhang, J.-J. Luo, X. Lin, M. Balmaseda, G. Wang, and B. J. Henley, 2021. Decadal climate variability in the tropical Pacific: Characteristics, causes, predictability, and prospects. *Science* 374(6563). DOI: 10.1126/science.aay9165.

QGIS Development Team, 2018. *QGIS Geographic Information System*. QGIS Association. http://www.qgis.org.

R Core Team, 2021. *R: A Language Environment for Statistical Computing*. R Foundation for Statistical Computing, Vienna, Austria. https://www.R-project.org/.

Robertson, C. S., 2011. *Dendroclimatology of yellow cedar (Callitropsis nootkatensis) in the Pacific Northwest of North America*. M.S. thesis, Western Washington University, Bellingham.

Salzer, M. W., M. K. Hughes, A. G. Bunn, and K. F. Kipfmueller, 2009. Recent unprecedented tree-ring growth in bristlecone pine at the highest elevations and possible causes. *Proceedings of the National Academy of Sciences* 106: 20348–20353.

Schneider, L., J. E. Smerdon, U. Büntgen, R. J. Wilson, V. S. Myglan, A. V. Kirdyanov, and J. Esper, 2015. Revising midlatitude summer temperatures back to AD 600 based on a wood density network. *Geophysical Research Letters* 42: 4556–4562.

Schurer, A. P., S. F. B. Tett, and G. C. Hegerl, 2014. Small influence of solar variability on climate over the past millennium. *Nature Geoscience* 7:104–108.

Shi, J., Y. Liu, E. A. Vaganov, J. Li, and Q. Cai, 2008. Statistical and process-based modeling analyses of tree growth response to climate in semi-arid area of north central China: A case study of *Pinus tabulaeformis*. *Journal of Geophysical Research: Biogeosciences* 113:G01026. https://doi.org/10.1029/2007JG000547.

St. George, S., 2014. An overview of tree-ring width records across the Northern Hemisphere. *Quaternary Science Reviews* 95:132–150.

Stephenson, N. L., 1998. Actual evapotranspiration and deficit: Biologically meaningful correlates of vegetation distribution across spatial scales. *Journal of Biogeography* 25:855–870.

Stoffel, M., M. Khodri, C. Corona, S. Guillet, V. Poulain, S. Bekki, J. Guiot, B. H. Luckman, C. Oppenheimer, N. Lebas, M. Beniston, and V. Masson-Delmotte, 2015. Estimates of volcanic-induced cooling in the Northern Hemisphere over the past 1,500 years. *Nature Geoscience* 8:784–788.

Stokes, M. A., and T. L. Smiley, 1968. *An Introduction to Tree-Ring Dating*. The University of Arizona Press, Tucson.

Tardif, J., M. Salzer, F. Conciatori, A. Bunn, and M. Hughes, 2020. Formation, structure and climatic significance of blue rings and frost rings in high elevation bristlecone pine (*Pinus longaeva* D.K. Bailey). *Quaternary Science Reviews* 244:106516. https://doi.org/10.1016/j.quascirev.2020.106516.

Trinies, C. A., 2019. *Dendroclimatology of Yellow Cedar (*Callitropsis nootkatensis*) and Late Holocene Temperature Variability on the Western Slopes of the North Cascades in Washington State*. M.S. thesis, Western Washington University, Bellingham.

Trouet, V., H. F. Diaz, E. R. Wahl, A. E. Viau, R. Graham, N. E. Graham, and E. R. Cook, 2013. A 1500-year reconstruction of annual mean temperature for temperate North America on decadal-to-multidecadal time scales. *Environmental Research Letters* 8(2):024008. doi:10.1088/1748-9326/8/2/024008.

Vaganov, E. A., K. J. Anchukaitis, and M. N. Evans, 2011. How well understood are the processes that create dendroclimatic records? A mechanistic model of the climatic control on conifer tree-ring growth dynamics. In *Dendroclimatology*, edited by Hughes, M., T. Swetnam, and H. Diaz, pp. 37–75. Springer, Netherlands.

Vaganov, E., M. Hughes, A. Kirdyanov, F. Schweingruber, and P. Silkin, 1999. Influence of snowfall and melt timing on tree growth in subarctic Eurasia. *Nature* 400:149–151.

Vaganov, E. A., M. K. Hughes, and A. V. Shashkin, 2006. Environmental control of xylem differentiation. In *Growth Dynamics of Conifer Tree Rings*, pp. 151–187. Ecological Studies, v. 183, Springer, Berlin, Heidelberg. https://doi.org/10.1007/3-540-31298-6_6.

Wettstein, J. J., J. S. Littell, J. M. Wallace, and Z. Gedalof, 2011. Coherent region-, species-, and frequency-dependent local climate signals in Northern Hemisphere tree-ring widths. *Journal of Climate* 24:5998–6012.

Wiles, G. C., J. Charlton, R. J. Wilson, R. D. D'Arrigo, B. Buma, J. Krapek, B. V. Gaglioti, N. Wiesenberg, and R. Oelkers, 2019. Yellow-cedar blue intensity tree-ring chronologies as records of climate in Juneau, Alaska, USA. *Canadian Journal of Forest Research* 49:1483–1492.

Wiles, G. C., C. R. Mennett, S. K. Jarvis, R. D. D'Arrigo, N. Wiesenberg, and D. E. Lawson, 2012. Tree-ring investigations into changing climatic responses of yellow-cedar, Glacier Bay, Alaska. *Canadian Journal of Forest Research* 42:814–819.

Williams, A. P., J. Michaelsen, S. W. Leavitt, and C. J. Still, 2010. Using tree rings to predict the response of tree growth to climate change in the continental United States during the twenty-first century. *Earth Interactions* 14:1–20.

Wilson, R., K. Anchukaitis, L. Andreu-Hayles, E. Cook, R. D'Arrigo, N. Davi, L. Haberbauer, P. Krusic, B. Luckman, D. Morimoto, R. Oelkers, G. Wiles, and C. Wood, 2019. Improved dendroclimatic calibration using blue intensity in the southern Yukon. *The Holocene* 29:1817–1830.

Wilson, R., R. D'Arrigo, L. Andreu-Hayles, R. Oelkers, G. Wiles, K. Anchukaitis, and N. Davi, 2017. Experiments based on blue intensity for reconstructing North Pacific temperatures along the Gulf of Alaska. *Climate of the Past* 13:1007–1022.

Wilson, R. J. S., K. J. Anchukaitis, K. R. Briffa, U. Büntgen, E. R. Cook, R. D. D'Arrigo, N. Davi, J. Esper, D. C. Frank, B. E. Gunnarson, G. C. Hegerl, S. Helama, S. Klesse, P. J. Krusic, H. W. Linderholm, V. Myglan, T. J. Osborn, M. Rydval, L. Schneider, A. Schurer, G. C. Wiles, P. Zhang, and E. Zorita, 2016. Last millennium Northern Hemisphere summer temperatures from tree rings: Part I: The long term context. *Quaternary Science Reviews* 134:1–18.

Zang, C., and F. Biondi, 2015. Treeclim: An R package for the numerical calibration of proxy-climate relationships. *Ecography* 38:431–436.

*Received 27 October 2021; accepted 12 April 2022.*